

Quantum Monte Carlo study of the two-dimensional electron gas in presence of Rashba interaction

A. Ambrosetti,^{*} F. Pederiva,[†] and E. Lipparini[‡]

*Dipartimento di Fisica, University of Trento, Via Sommarive 14, Povo, I-38123 Trento, Italy
and INFN, Gruppo Collegato di Trento, I-38123 Trento, Italy*

S. Gandolfi[§]

*International School for Advanced Studies (SISSA), Via Beirut 2/4, I-34014 Trieste, Italy
and INFN, Sezione di Trieste, I-34014 Trieste, Italy*

(Received 8 May 2009; revised manuscript received 6 August 2009; published 11 September 2009)

We introduce a variant to the diffusion Monte Carlo algorithm that can be employed to study the effects of the Rashba interaction in many-electron systems. Because of the spin-orbit nature of Rashba interaction a standard algorithm cannot be applied and therefore a specific imaginary time spin-dependent propagator has been developed and implemented following previous work developed in the framework of nuclear physics. We computed the ground-state energy of the two-dimensional electron gas at different densities for several values of the Rashba interaction strength as a function of “Rashba spin states” polarization. Comparison is given with analytically known Hartree-Fock results and for the system in absence of Coulomb interaction.

DOI: [10.1103/PhysRevB.80.125306](https://doi.org/10.1103/PhysRevB.80.125306)

PACS number(s): 71.10.Ca, 73.21.Fg

I. INTRODUCTION

The Rashba interaction, an electric-field-induced spin-orbit coupling, has been experimentally observed in semiconductor heterostructures, depending on their symmetry, and has been proved to be tunable in strength through a gate voltage.^{1,2} The external voltage can then be used to control the spin state of the system. This property becomes extremely interesting in view of spintronics applications. Several experiments have also been performed with the aim of studying the dependence of the interaction strength on applied gate voltage and well thickness.³

The typical experimental setup consists of a device etched on a two-dimensional (2D) quantum well formed at the interface of two semiconductors. In such devices electrons are constrained to move in a two-dimensional space ($O\hat{x}-O\hat{y}$) forming a 2D gas. The asymmetry of the quantum well generates an electric field, along the \hat{z} direction, perpendicular to the plane containing the electrons. This causes electrons to be subject to an effective magnetic field $\mathbf{B}_{\text{eff}} \propto \mathbf{p} \times \mathbf{E}$ coupling to their spin. Such coupling gives rise to the well-known Rashba potential,⁴

$$V_{\text{Rashba}} = \lambda \sum_{i=1}^N [p_i^y \sigma_i^x - p_i^x \sigma_i^y], \quad (1)$$

where \mathbf{p}_i is the momentum of the i th electron, and σ_i^x and σ_i^y are the Pauli matrices acting over the spin of particle i . Neglecting the Coulomb interaction among the electrons the Hamiltonian is a sum of one body terms, and the problem is analytically solvable. Single particle solutions are given by plane waves with \mathbf{k} -dependent spinors. In particular, for each wave vector with momentum \mathbf{k} two possible solutions exist,

$$\chi(\mathbf{r}) = \frac{e^{i\mathbf{k}\cdot\mathbf{r}}}{\sqrt{2}} \begin{pmatrix} \pm \frac{k_y + ik_x}{k} \\ 1 \end{pmatrix}. \quad (2)$$

These solutions correspond to two different spin states, with the following dispersion law:

$$\varepsilon(k)_{\pm} = \frac{\mathbf{k}^2}{2m} \pm \lambda |\mathbf{k}|. \quad (3)$$

This spin splitting causes noninteracting electrons to arrange in two bands with different fillings depending on the interaction strength λ , therefore inducing a natural imbalance in the filling of the two bands. In this case two different Fermi surfaces are generated, as also shown experimentally by beating patterns in the Shubnikov–De Haas oscillations.^{1,2} We will refer to this unbalance as to a “Rashba spin-state” (RSS) polarization. Being λ proportional to the intensity of the external electric field, it is possible to manipulate the occupation numbers and to induce at the same time precession on the electron spin. These properties induced studies in the direction of spin field effect transistors.⁵

Once the Coulomb interaction is included in the Hamiltonian, no analytic solution is available. Several methods can be used to study this system and much theoretical work has been done so far (for a review see, e.g., Ref. 6). The Hartree-Fock (HF) method gives a simple analytical solution, and though it totally ignores the effect of correlations, it provides a useful insight on the structure of the single-particle levels. Another interesting approach consists in applying a unitary transformation U (Refs. 7 and 8) giving, to leading order in the spin-orbit strength, a transformed Hamiltonian $\tilde{H} = U^{-1} H U$ whose eigenstates are also spin and angular-momentum eigenstates. Though approximate, this method allows the use of standard Quantum Monte Carlo techniques.⁹

In this work a particular implementation of the diffusion Monte Carlo (DMC), directly dealing with spin-orbit interactions, is proposed in order to obtain an *ab initio* method giving accurate ground-state energies of the system. No transformation is needed because the spin-orbit term is included in the imaginary time propagator.

The paper is organized as follows: in Sec. II we describe the diffusion Monte Carlo method and the way in which the Green’s function used for treating Rashba interaction is derived. The trial wave function used as a starting point for the

projection is described in Sec. II C. Finally in Sec. III the results are presented and discussed together with Hartree-Fock energies for the ground state of the system,¹⁰ and conclusions are given in Sec. IV.

II. METHOD

A. Diffusion Monte Carlo method for general spin-independent many-body problems

The DMC method is based on imaginary time evolution projection. Through the use of an appropriate Green's function, an initial state is projected over its lowest energy component having the same nodes or the same phase as the trial wave function ψ_T . Given an initial wave function $\psi(\mathbf{R}, 0)$ its propagation in imaginary time τ is given by

$$\begin{aligned} \psi(\mathbf{R}, \tau) &= \exp[-(H - E_0)\tau]\psi(\mathbf{R}, 0) \\ &= \sum_n c_n \exp[-(H - E_0)\tau]\phi_n(\mathbf{R}), \end{aligned} \quad (4)$$

where E_0 is a normalization factor, $\phi_n(\mathbf{R})$ are the eigenstates of the Hamiltonian, and \mathbf{R} represents the space coordinates of the system. The amplitudes of higher energy states, due to propagation, decay exponentially with τ , with a lifetime inversely proportional to their energy relative to E_0 . If $\psi(\mathbf{R}, 0)$ is not orthogonal to the ground state, $\psi(\mathbf{R}, \tau \rightarrow \infty)$ will be proportional to the ground state itself.

A typical many-body system is described with a Hamiltonian of the form

$$H = \hat{T} + \hat{V}, \quad (5)$$

where \hat{T} is the sum of single-particle kinetic-energy operators, and the potential \hat{V} between all the electrons only depends on spatial coordinates. The evolution in imaginary time can be achieved by means of the Green's function of the Hamiltonian that can be approximated by using Trotter's formula,

$$e^{-\tau\hat{H}} = e^{-\tau\hat{V}}e^{-\tau\hat{T}} + o(\tau^2). \quad (6)$$

In space representation propagator (6) can be written as

$$G(\mathbf{R}, \mathbf{R}', \tau) = \langle \mathbf{R} | e^{-(\hat{H}-E_0)\tau} | \mathbf{R}' \rangle \simeq e^{-[V(\mathbf{R})-E_0]\tau} G_0(\mathbf{R}, \mathbf{R}', \tau). \quad (7)$$

G_0 is the exact Green's function of a two-dimensional non-interacting system:

$$G_0(\mathbf{R}, \mathbf{R}', \tau) = \frac{1}{4\pi D\tau} e^{-[(\mathbf{R} - \mathbf{R}')^2/2D\tau]}, \quad (8)$$

where $D = \hbar^2/m$ is the diffusion constant. The exponential of the kinetic term gives rise to a free particle imaginary time Green's function G_0 , while the other term is viewed as a weighting term.

The algorithm makes use of walkers, i.e., points in the coordinate space, in order to sample the ground-state wave function. The propagation is obtained by diffusing the walkers according the displacements distribution given by G_0 .

Afterwards a weight is assigned to the walkers according to the other factor in the propagator given by the potential energy of the system. Because of the Trotter approximation, the Green's function is correct only at order $O(\tau)$. The problem is overcome by using short-time propagation repeatedly in order to achieve long enough imaginary times and adequate statistics, minimizing at the same time the time step error. The result is given after an extrapolation to $\Delta\tau \rightarrow 0$.

In order to enhance the efficiency, importance sampling is implemented in DMC algorithms.^{11,12} The idea consists in sampling a density of points proportional to the ground-state distribution multiplied by an importance function. In standard cases the importance function will only depend on space coordinates being the spin fixed; thus,

$$\psi_T(\mathbf{R})\phi(\mathbf{R}, \tau) = \int G(\mathbf{R}, \mathbf{R}', \tau) \frac{\psi_T(\mathbf{R})}{\psi_T(\mathbf{R}')} \psi_T(\mathbf{R}')\phi(\mathbf{R}', 0) d\mathbf{R}'. \quad (9)$$

This can be shown to introduce a drift in G_0 and to modify the weighting factor, which will not only contain the potential, but also the local energy $E_L = H\psi_T(\mathbf{R})/\psi_T(\mathbf{R})$ of the system.

B. Many-body spin-dependent Hamiltonian

The system we are studying is a two-dimensional electron gas at $T=0$, in presence of both Coulomb and Rashba interaction, with the addition of a uniform charge background.^{13,14} The Hamiltonian for the system can be written as

$$H = \sum_{i=1}^N \frac{p_i^2}{2m} + \lambda \sum_{i=1}^N (p_i^y \sigma_i^x - p_i^x \sigma_i^y) + V_{Coul}(\mathbf{R}), \quad (10)$$

where V_{Coul} includes the electron-electron interaction and the effects of the background. The Hamiltonian in this case does not only contain space coordinate dependent potentials. The Rashba interaction, because of its spin-orbit character, contains spin and momentum operators, which therefore cannot be treated like simple weighting factors as in the case shown above. In order to apply the DMC technique, a new propagator form is needed, taking into account the particular features of nonlocality and spin dependence.^{15,16}

In order to simplify the following calculations let us first consider the single-particle Hamiltonian given by the kinetic term and the Rashba interaction for only one electron. By applying Trotter's formula the following form of the Green's function can be obtained,

$$G(\mathbf{r}, \mathbf{r}', \Delta\tau) = e^{-\lambda(p_y \sigma_x - p_x \sigma_y)\Delta\tau} G_0(\mathbf{r}, \mathbf{r}', \Delta\tau), \quad (11)$$

where the Pauli matrices σ_x and σ_y act on the spin components of the electron, and \mathbf{r} and \mathbf{r}' are the coordinates of the electron after and before the diffusion generated by G_0 . The last factor G_0 will again give the space displacement, while the second one, including the Rashba interaction, contains both momentum and spin operators, and can be viewed as acting on the free propagator. Expanding to first order in $\Delta\tau$ the first factor of Eq. (11), and applying the derivatives given by $\mathbf{p} = -i\hbar\nabla$ to G_0 , we have

$$\begin{aligned} & \left[1 - i \frac{\lambda}{D} (\sigma_x \Delta y - \sigma_y \Delta x) \right] G_0(\mathbf{r}, \mathbf{r}', \Delta \tau) \\ & \simeq \exp \left[-i \frac{\lambda}{D} (\sigma_x \Delta y - \sigma_y \Delta x) \right] G_0(\mathbf{r}, \mathbf{r}', \Delta \tau). \end{aligned} \quad (12)$$

The first part can be interpreted as a spin rotation depending on $\Delta x = x - x'$ and $\Delta y = y - y'$, i.e., the displacement generated by the Gaussian free particle Green's function G_0 . The appearance of the spin-rotating factor in the Green's function implies that the spin coordinates of the electrons must be explicitly used. Making use of a spinorial representation, the spin state for the i th electron is given by

$$|s_i\rangle = \alpha_i |\uparrow\rangle + \beta_i |\downarrow\rangle, \quad (13)$$

where α and β are the amplitudes of the spin state in the $\{|\uparrow\rangle\}$ and $\{|\downarrow\rangle\}$ basis.

The propagation of the spin-dependent Green's function can then be realized with a rotation of spinors. For each electron i the spin-dependent propagator can be written using the following matrix form:

$$\begin{aligned} & \exp \left[-i \frac{\lambda}{D} (\sigma_x \Delta y - \sigma_y \Delta x) \right] \\ & \equiv O_i \\ & = \begin{pmatrix} \cos\left(\frac{\lambda}{D} \Delta r_i\right) & \sin\left(\frac{\lambda}{D} \Delta r_i\right) \frac{-i \Delta y_i + \Delta x_i}{\Delta r_i} \\ -\sin\left(\frac{\lambda}{D} \Delta r_i\right) \frac{i \Delta y_i + \Delta x_i}{\Delta r_i} & \cos\left(\frac{\lambda}{D} \Delta r_i\right) \end{pmatrix}, \end{aligned} \quad (14)$$

where $\Delta r_i = \sqrt{\Delta x_i^2 + \Delta y_i^2}$. Therefore, during the propagation in imaginary time, an electron with initial coordinates $(\mathbf{r}_i, \alpha_i, \beta_i)$, will be first moved to $(\mathbf{r}'_i, \alpha_i, \beta_i)$ due to the free propagator G_0 , and then to $(\mathbf{r}'_i, \alpha'_i, \beta'_i)$ due to rotation according to

$$(\alpha'_i, \beta'_i) = O_i \begin{pmatrix} \alpha_i \\ \beta_i \end{pmatrix}. \quad (15)$$

The approximations introduced after Eq. (11) generate an error, which must be now taken into account at least to order $\Delta \tau$. If the spin-orbit propagator just derived were correct, we would expect to obtain

$$\begin{aligned} & \int e^{-i\lambda/D(\sigma_x \Delta y - \sigma_y \Delta x)} G_0(\mathbf{r}, \mathbf{r}', \Delta \tau) \psi(\mathbf{r}') d\mathbf{r}' \\ & = e^{-\lambda(p_y \sigma_x - p_x \sigma_y)} \int G_0(\mathbf{r}, \mathbf{r}', \Delta \tau) \psi(\mathbf{r}') d\mathbf{r}'. \end{aligned} \quad (16)$$

This equation does not hold unless the propagator is corrected for a weighting factor,

$$e^{(\lambda^2/D)\Delta \tau}. \quad (17)$$

It is important to note that the results obtained following this approach coincide with the analytical form of the Green's function for the system in absence of Coulomb potential. In this case no error is introduced in $G(\mathbf{R}, \mathbf{R}', \Delta \tau)$ because the

Rashba interaction commutes with the kinetic term of the Hamiltonian.

By considering the full many-particle Hamiltonian, including the Coulomb interaction, the total Green's function is

$$\begin{aligned} G(\mathbf{R}, \mathbf{R}', \Delta \tau) & = e^{-[V_{Coul}(\mathbf{R}) - E_0 - N\lambda^2/D]\Delta \tau} \\ & \times e^{-i\lambda/D \sum_{i=1}^N (\Delta r_i^y \sigma_i^x - \Delta r_i^x \sigma_i^y) \Delta \tau} G_0(\mathbf{R}, \mathbf{R}', \Delta \tau). \end{aligned} \quad (18)$$

When a spin-orbit term is introduced in the Hamiltonian, as shown before, the propagator will not leave spin unchanged because space coordinate diffusion becomes related to spin rotation. This means that also the importance sampling should not be naively applied, but in the total weight, a factor $\psi_T(\mathbf{R}, S) / \psi_T(\mathbf{R}', S')$, where S' and S respectively are the old and new spin states, should be taken into account. It is possible to apply the importance sampling adding a drift term in G_0 as usual by considering

$$\frac{\psi_T(\mathbf{R}, S)}{\psi_T(\mathbf{R}', S')} = \frac{\psi_T(\mathbf{R}, S')}{\psi_T(\mathbf{R}', S')} \frac{\psi_T(\mathbf{R}, S)}{\psi_T(\mathbf{R}, S')} \approx \frac{\psi_T(\mathbf{R}, S')}{\psi_T(\mathbf{R}', S')} \frac{\psi_T(\mathbf{R}', S)}{\psi_T(\mathbf{R}', S')}, \quad (19)$$

where the two forms of Eq. (19) are equivalent to first order in $\Delta \tau$. The factor where spins are unchanged can be included as usual, while the second one can be interpreted as an additional weighting factor. We point out that in this case the local energy appearing in the weight includes only the spin-independent part of the Hamiltonian.

C. Wave function

We used a trial wave function made of a Slater determinant of single-particle states multiplied by a Jastrow factor accounting for correlations, according to the form

$$\psi_T(\mathbf{R}, S) = D(\mathbf{R}, S) \exp \left(- \sum_{i < j}^N u(|\mathbf{r}_i - \mathbf{r}_j|) \right), \quad (20)$$

where $u(r)$ is a two-body pseudopotential of the double Yukawa form.^{13,14}

Single-particle states used to build the determinant are chosen as the eigenstates of the Hamiltonian in absence of Coulomb interaction, coinciding also with Hartree-Fock single-particle solutions, written in Eq. (2)

$$\phi_{\mathbf{k}, \pm}(\mathbf{r}, \alpha, \beta) = \left[\pm \alpha \frac{k_y + ik_x}{|\mathbf{k}|} + \beta \right] e^{i\mathbf{k} \cdot \mathbf{r}}, \quad (21)$$

where α and β are, respectively, the up- and down-spin components with respect to the z axis. These are pairs of wave functions which we will call *quasiup* (plus sign) and *quasidown* (minus sign) states.

DMC simulations of infinite systems are usually performed in close shell configurations in order to obtain a real wave function and to reduce the finite-size effects mainly due to the kinetic energy. This makes it possible to apply the fixed node approximation in order to obtain a state with the same symmetry as ψ_T . In our case the trial wave function cannot be reduced to a real form because of the phase change

induced by spin rotation. Therefore we employ the fixed-phase approximation.¹⁶⁻²¹ For any complex wave function it is always possible to factorize the modulus in the following way:

$$\psi_T(\mathbf{R}, S) = |\psi_T(\mathbf{R}, S)| e^{i\theta_T(\mathbf{R}, S)}. \quad (22)$$

Using fixed node approximation means finding the lowest energy state $\phi(\mathbf{R})$ whose product with the (in this case real) trial wave function is positively defined $\phi(\mathbf{R})\psi_T^*(\mathbf{R}) = \phi(\mathbf{R})\psi_T(\mathbf{R}) > 0$. In our case this product does not have a defined sign and cannot be used as a sampling density,

$$\begin{aligned} \phi(\mathbf{R}, S)\psi_T^*(\mathbf{R}, S) \\ = |\phi(\mathbf{R}, S)| |\psi_T(\mathbf{R}, S)| \exp[i(\theta(\mathbf{R}, S) - \theta_T(\mathbf{R}, S))]. \end{aligned} \quad (23)$$

In the fixed phase approximation the problem is overcome assuming

$$\exp[i(\theta(\mathbf{R}, S) - \theta_T(\mathbf{R}, S))] = 1, \quad (24)$$

which corresponds to finding a solution with the same phase as the trial wave function. Under this assumption Eq. (23) becomes positive definite and the sampled distribution will only depend on the wave-function modulus.

In order to calculate the ground-state energy at different RSS polarizations and to reduce finite-size effects, twist averaged boundary conditions (TABCs) have been introduced in the algorithm.^{16,22} As shown in the electron gas without spin-orbit interactions, this allows to obtain good results without the need to use a very large number of electrons, giving therefore a great improvement in terms of the computational time required.

III. RESULTS

In order to verify our method a check has been performed by comparing numerical results with the exact solution obtained neglecting the electron-electron interaction. As mentioned in the introduction, the Hamiltonian

$$H_0 = \sum_{i=1}^N \frac{p_i^2}{2m} + \lambda \sum_{i=1}^N [p_i^y \sigma_i^x - p_i^x \sigma_i^y] \quad (25)$$

can be diagonalized by the single-particle wave functions [Eq. (21)]. The analytical solution to N fermions only subject to Rashba interaction is therefore a $N \times N$ Slater determinant of these single-particle solutions. For a given λ value, the ground state has a well defined RSS polarization. As a test for our DMC we multiplied the exact wave function by a Slater determinant in order to obtain a wrong state with the same nodes as the real ground state. Our algorithm indeed proved to be able to project out the ground state obtaining the analytical result within error bars.

In this work we make use of the dimensionless parameter $r_s = r_0/a_0$, defined as a function of the Bohr radius $a_0 = \hbar^2/m_e^2$ and the radius containing only one particle on average $V/N = \pi r_0^2$. Energies are given in units of Rydberg/electron (1 Ry = $e^2/2a_0$) and the Hamiltonian of Eq. (10) in these units is

$$H = \sum_{i=1}^N \left[\frac{-\nabla_i^2}{r_s^2} - \frac{2i\lambda}{r_s} (\partial_i^y \sigma_i^x - \partial_i^x \sigma_i^y) \right] + \quad (26)$$

$$\frac{2e^2}{r_s} \sum_{i < j}^N \frac{1}{|\mathbf{r}_i - \mathbf{r}_j|} + V_{back}, \quad (27)$$

where V_{back} contains the effects of the charge background.

The main numerical results presented in this work concern the ground-state energies of the two-dimensional electron gas with Coulomb and Rashba interaction at different densities (expressed in terms of the r_s parameter), different values of the intensity λ of the Rashba interaction and different RSS polarizations defined as

$$\xi = \frac{N_+ - N_-}{N}, \quad (28)$$

where N_- and N_+ are the numbers of electrons in the quasideown- and quasiup-spin states respectively, and the total number of electrons in the simulation is fixed to $N=58$. All the values obtained for the ground-state energies as a function of r_s , λ , and ξ are reported in the Appendix, where the DMC and the Hartree-Fock results are compared.

In particular the r_s values 1, 5, 10, and 20 were chosen and, for each density, calculations were performed at different λ values of ground-state energy as a function of quasiup-quasideown occupation numbers, the total number of electrons in our simulation being fixed to $N=58$. Simulations were done for relatively low values of r_s , distant from the Wigner crystallization regime. Calculations would also be possible for lower densities given an appropriate set of single-particle orbitals. This might be achieved by linear combination of Hartree-Fock orbitals, in order to obtain a wave function of the same quality as that used in the gas phase. Coulomb interaction was treated by means of the Ewald sums.²³ As a comparison, besides DMC results, we also give Hartree-Fock energies, which are given, in this case, by the following analytic form for infinite systems:

$$\begin{aligned} \frac{E}{N} = \frac{(1 - \xi^2)}{r_s^2} + \frac{2\sqrt{2}}{r_s^3} \\ \times \left[\left(\lambda - \frac{2}{\pi} \right) (1 + \xi)^{3/2} - \left(\lambda + \frac{2}{\pi} \right) (1 - \xi)^{3/2} \right]. \end{aligned} \quad (29)$$

where ξ was defined in Eq. (28).

DMC results at nonzero RSS polarization are obtained by projecting out of a trial wave function ψ_T whose Slater determinant contains different numbers of *quasiup-* and *quasideown-*spin states. The approach is apparently similar to what is commonly done for the electron gas in absence of spin-orbit interaction. However, in this case the Hamiltonian does not commute with the z spin component. The choice of the quasiup and quasideown basis was made by comparison with the results obtained using the standard spin-up and spin-down basis. The latter consistently gives higher values of the energy for the ground-state RSS polarization. Results in absence of Coulomb interaction predict spin-state RSS polarization as a consequence of a two band dispersion law. A

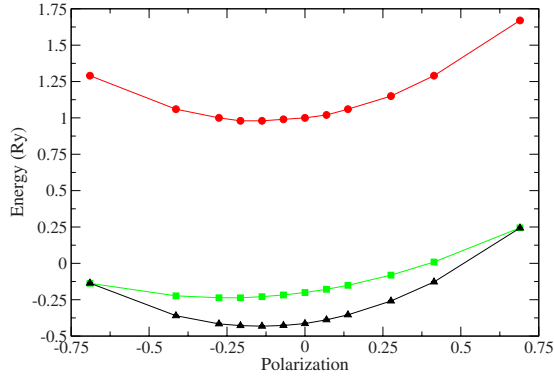


FIG. 1. (Color online) Energy values at $r_s=1$ and $\lambda=0.1$, respectively, obtained with DMC (triangles), HF (squares), and without Coulomb interaction (circles).

very similar behavior for the energy as a function of RSS polarization is found in our results (see Fig. 1). This suggests the existence of an analogous two band structure also in presence of Coulomb interaction as experimentally proved by the Shubnikov–De Haas oscillations.

In Fig. 2 energies at different λ are shown as a function of the RSS polarization ξ . As expected, the RSS polarization depends on the intensity of the spin-orbit interaction, increasing in module with larger λ . Calculations have been performed at different r_s values, corresponding to different densities. The onset of RSS polarization occurs at lower and lower strengths of the Rashba interaction when the density is decreased. This is an effect of the Rashba interaction dependence on the momentum. In the Hamiltonian of Eq. (27) the $1/r_s$ prefactors for the interaction terms, compared to the $1/r_s^2$ of the kinetic energy let interactions become more efficient at high r_s (low density) compared to the kinetic term. While at high density the system will look less interacting, and therefore also less polarized, at larger values of r_s the system will be more sensitive to the spin-orbit interaction and will be more polarized also for smaller λ .

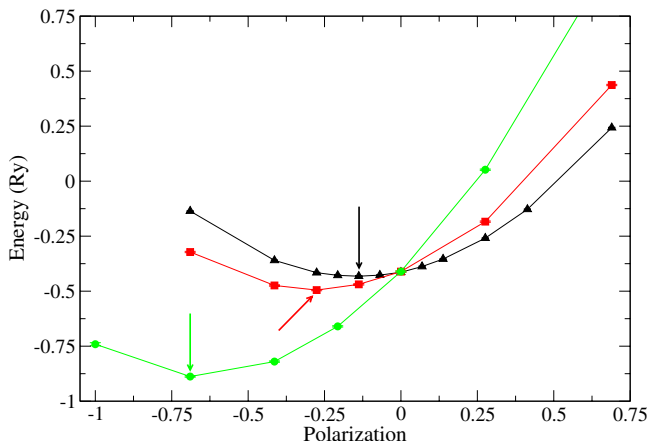


FIG. 2. (Color online) Energy values obtained at $r_s=1$ for three different λ values, respectively, 0.1 (triangles), 0.2 (squares), and 0.5 (circles). The arrows indicate the point of minimum energy for each λ . For increasing λ the energy minimum shifts to larger (in modulus) RSS polarization.

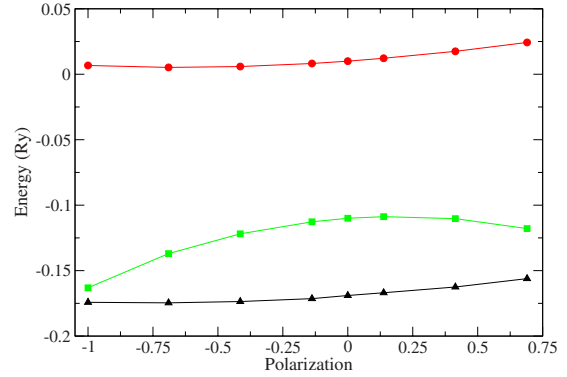


FIG. 3. (Color online) Energy values at $r_s=10$ $\lambda=0.05$ as in the figure above. DMC results are represented by triangles, HF by squares and results in absence of Coulomb interaction by circles.

At lower densities correlations among electrons play a major role. In Figs. 1 and 3 DMC energies are shown together with the corresponding results from HF approximation. We see a worsening agreement when r_s increases. This must be due to the fact that HF approximation does not take correlations into account, causing a larger deviation when the N electrons wave function becomes less similar to a Slater determinant.

In Fig. 4 energies for the 2D electron gas from Ref. 24 are compared with ground-state results in presence of spin-orbit interaction with fixed strength $\lambda=0.1$. In presence of Rashba interaction ground states have a different structure and their RSS polarization varies with the density. However the ground-state energy is always lower than in absence of spin-orbit interaction over the whole density range.

In Fig. 5 the pair-correlation function $g(r)$ decomposed into triplet and singlet components is reported. Triplet and singlet components were obtained collecting the following quantities:

$$g_c(r) = N \sum_{i < j} \frac{\langle \psi_T | \delta(r_{ij} - r) | \psi_T \rangle}{\langle \psi_T | \psi_T \rangle} \quad (30)$$

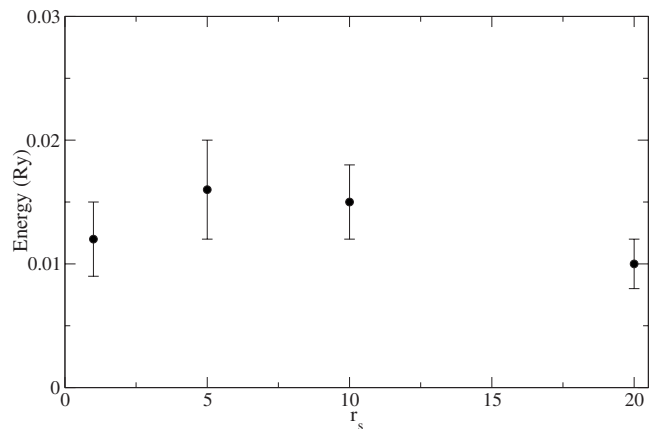


FIG. 4. Difference between energies without and in presence of Rashba interaction ($\lambda=1$). Data were taken from Ref. 24.

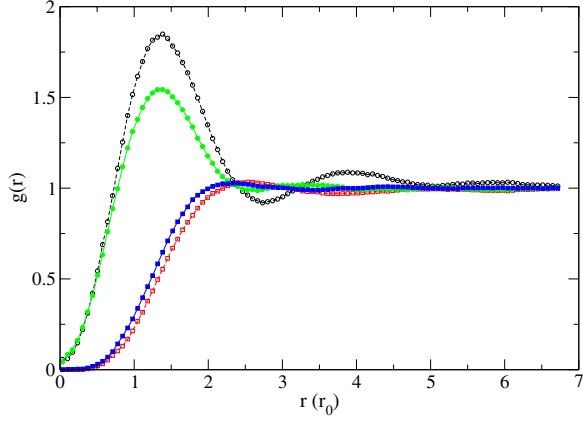


FIG. 5. (Color online) Pair correlation function $g(r)$ decomposed into singlet (circles) and triplet (squares) channels for $r_s=5$ with (closed symbols) and without (open symbols) spin-orbit interaction. For better comparison the curves are all normalized to give $g(r) \rightarrow 1$ for $r \rightarrow \infty$.

$$g_\sigma(r) = N \sum_{i < j} \frac{\langle \psi_T | \delta(r_{ij} - r) \boldsymbol{\sigma}_i \cdot \boldsymbol{\sigma}_j | \psi_T \rangle}{\langle \psi_T | \psi_T \rangle} \quad (31)$$

where N is a normalization factor, and composing them according to the triplet and singlet spin projectors,¹⁶

$$g_{S=0}(r) = \frac{1}{4} [g_c(r) - g_\sigma(r)], \quad (32)$$

$$g_{S=1}(r) = \frac{1}{4} [3g_c(r) + g_\sigma(r)]. \quad (33)$$

The results show a tendency for the triplet and singlet first peaks to become smaller and closer to each other when spin-orbit interaction is switched on. This suggests a decrease in the antiferromagnetic character of the electrons, probably due to the induced RSS polarization.

IV. CONCLUSIONS

We have implemented a DMC algorithm for treating Rashba spin-orbit interaction in the electron gas. We have calculated the equation of state of 2D electron gas in the presence of Rashba interaction. We computed the energy per particle as a function of the strength λ of the Rashba potential, r_s and the RSS polarization ξ showing system RSS polarization and comparing the results with analytical HF results. Our work not only gives results for the 2D electron gas but also provides a good test for the algorithm, opening new possibilities for implementation on other systems, in particular quantum dots or quantum wires involving both the Rashba and the Dresselhaus potential.²⁵ A similar treatment can also be extended to finite systems such as atoms and molecules.

ACKNOWLEDGMENTS

This work was partially supported by INFM. Computer calculations were performed on the WIGLAF cluster of

the Department of Physics, University of Trento, on the BEN cluster at ECT* in Trento, and also using CINECA resources.

APPENDIX: TABLES WITH RESULTS

In Tables I–IV the diffusion Monte Carlo results are reported together with corresponding Hartree-Fock energies and results for the system without the Coulomb interaction with the Rashba interaction only.

TABLE I. Energies of the system at $r_s=1$ and $\lambda=0.1, 0.2$, and 0.5 for various RSS polarizations ξ as defined in Eq. (28). The DMC result is computed with Coulomb and Rashba interaction, E_{Rashba} is the energy given by Rashba Hamiltonian (25), and in the last column the Hartree-Fock result is reported. All the energies are expressed in Ry.

ξ	N_-	N_+	E_{DMC}	E_{Rashba}	E_{HF}
$\lambda=0.1$					
0.690	9	49	0.243(4)	1.67	0.244
0.414	17	41	-0.128(3)	1.29	0.009
0.276	21	37	-0.259(3)	1.15	-0.081
0.138	25	33	-0.354(2)	1.06	-0.151
0.069	27	31	-0.388(4)	1.024	-0.178
0.0	29	29	-0.414(3)	1.00	-0.200
-0.069	31	27	-0.427(4)	0.985	-0.217
-0.138	33	25	-0.432(3)	0.98	-0.229
-0.207	35	23	-0.428(3)	0.984	-0.235
-0.276	37	21	-0.416(5)	0.998	-0.237
-0.414	41	17	-0.360(4)	1.06	-0.223
-0.690	49	9	-0.136(4)	1.29	-0.137
$\lambda=0.2$					
0.690	9	49	0.437(4)	1.86	0.435
0.414	17	41	-0.008(4)	1.40	0.125
0.276	21	37	-0.184(5)	1.23	-0.022
0.138	25	33	-0.306(5)	1.1	-0.112
0.0	29	29	-0.411(4)	1.00	-0.200
-0.138	33	25	-0.469(3)	0.94	-0.268
-0.276	37	21	-0.514(5)	0.92	-0.314
-0.414	41	17	-0.474(5)	0.94	-0.340
-0.690	49	9	-0.322(4)	1.09	-0.328
$\lambda=0.5$					
0.690	9	49	1.013(7)	2.43	1.008
0.276	21	37	0.053(6)	1.47	0.230
0.0	29	29	-0.410(6)	1.00	-0.200
-0.207	35	23	-0.660(3)	0.75	-0.469
-0.414	41	17	-0.821(5)	0.59	-0.688
-0.690	49	9	-0.888(8)	0.52	-0.900
-1.0	58	0	-0.741(7)	0.67	-1.031

TABLE II. Energies of the system at $r_s=5$ and $\lambda=0.02$ and 0.1 for various RSS polarizations ξ as defined in Eq. (28). The DMC result is computed with Coulomb and Rashba interaction, E_{Rashba} is the energy given by Rashba Hamiltonian (25), and in the last column the Hartree-Fock result is reported. All the energies are expressed in Ry.

ξ	N_-	N_+	E_{DMC}	E_{Rashba}	E_{HF}
$\lambda=0.02$					
0.690	9	49	-0.2719(5)	0.0667	-0.2178
0.414	17	41	-0.2861(5)	0.0515	-0.2042
0.138	25	33	-0.2947(5)	0.0423	-0.1995
0.0	29	29	-0.2971(5)	0.0400	-0.2001
-0.138	33	25	-0.2978(4)	0.0392	-0.2026
-0.414	41	17	-0.2951(5)	0.0422	-0.2125
-0.690	49	9	-0.2867(4)	0.0514	-0.2330
-1.0	58	0	-0.2748(5)	0.0693	-0.2702
$\lambda=0.1$					
0.690	9	49	-0.2403(5)	0.0972	-0.1872
0.414	17	41	-0.2668(4)	0.0701	-0.1856
0.138	25	33	-0.2879(4)	0.0486	-0.1932
0.0	29	29	-0.2964(4)	0.0400	-0.2001
-0.138	33	25	-0.3033(3)	0.0330	-0.2088
-0.414	41	17	-0.3127(3)	0.0236	-0.2321
-0.690	49	9	-0.3155(5)	0.0209	-0.2635
-1.0	58	0	-0.3099(5)	0.0267	-0.3129

TABLE III. Energies of the system at $r_s=10$ and $\lambda=0.02, 0.05,$ and 0.1 for various RSS polarizations ξ as defined in Eq. (28). The DMC result is computed with Coulomb and Rashba interaction, E_{Rashba} is the energy given by Rashba Hamiltonian (25), and in the last column the Hartree-Fock result is reported. All the energies are expressed in Ry.

ξ	N_-	N_+	E_{DMC}	E_{Rashba}	E_{HF}
$\lambda=0.02$					
0.690	9	49	-0.1621(5)	0.0186	-0.1236
0.414	17	41	-0.1660(2)	0.0140	-0.1138
0.138	25	33	-0.1688(3)	0.0110	-0.1099
0.0	29	29	-0.1694(2)	0.0100	-0.1100
-0.138	33	25	-0.1698(2)	0.0094	-0.1149
-0.414	41	17	-0.1700(2)	0.0094	-0.1184
-0.690	49	9	-0.1699(2)	0.0109	-0.1313
-1.0	58	0	-0.1684(3)	0.0147	-0.1551
$\lambda=0.05$					
0.690	9	49	-0.1561(4)	0.0243	-0.1179
0.414	17	41	-0.1625(3)	0.0175	-0.1103
0.138	25	33	-0.1669(3)	0.0122	-0.1088
0.0	29	29	-0.1690(2)	0.0100	-0.1100
-0.138	33	25	-0.1714(2)	0.0082	-0.1127
-0.414	41	17	-0.1736(2)	0.0059	-0.1219
-0.690	49	9	-0.1746(2)	0.0052	-0.1370
-1.0	58	0	-0.1742(2)	0.0067	-0.1631
$\lambda=0.1$					
0.690	9	49	-0.1459(4)	0.0338	-0.1084
0.414	17	41	-0.1565(3)	0.0233	-0.1045
0.138	25	33	-0.1656(3)	0.0141	-0.1068
0.0	29	29	-0.1696(2)	0.0100	-0.1100
-0.138	33	25	-0.1733(2)	0.0063	-0.1146
-0.414	41	17	-0.1792(2)	0.0001	-0.1277
-0.690	49	9	-0.1837(2)	-0.0043	-0.1465
-1.0	58	0	-0.1861(2)	-0.0067	-0.1764

TABLE IV. Energies of the system at $r_s=20$ and $\lambda=0.01, 0.02$, and 0.1 for various RSS polarizations ξ as defined in Eq. (28). The DMC result is computed with Coulomb and Rashba interaction, E_{Rashba} is the energy given by Rashba Hamiltonian (25), and in the last column the Hartree-Fock result is reported. All the energies are expressed in Ry.

ξ	N_-	N_+	E_{DMC}	E_{Rashba}	E_{HF}
$\lambda=0.01$					
0.690	9	49	-0.0901(3)	0.0046	-0.0665
0.414	17	41	-0.0912(2)	0.0035	-0.0604
0.138	25	33	-0.0919(2)	0.0027	-0.0577
0.0	29	29	-0.0921(2)	0.0025	-0.0575
-0.138	33	25	-0.0923(2)	0.0024	-0.0581
-0.414	41	17	-0.0923(3)	0.0023	-0.0616
-0.690	49	9	-0.0920(3)	0.0017	-0.0684
-1.0	58	0	-0.0912(4)	0.0037	-0.0812
$\lambda=0.02$					
0.690	9	49	-0.0892(2)	0.0056	-0.0655
0.414	17	41	-0.0906(2)	0.0041	-0.0598
0.138	25	33	-0.0918(3)	0.0029	-0.0575
0.0	29	29	-0.0922(2)	0.0025	-0.0575
-0.138	33	25	-0.0924(2)	0.0022	-0.0583
-0.414	41	17	-0.0928(2)	0.0018	-0.0622
-0.690	49	9	-0.0928(3)	0.0018	-0.0693
-1.0	58	0	-0.0924(5)	0.0023	-0.0825
$\lambda=0.1$					
0.690	9	49	-0.0811(3)	0.0132	-0.0579
0.414	17	41	-0.0856(2)	0.0087	-0.0552
0.0	29	29	-0.0918(2)	0.0045	-0.0560
-0.138	33	25	-0.0937(2)	0.0006	-0.0599
-0.414	41	17	-0.0972(2)	-0.0029	-0.0668
-0.690	49	9	-0.1001(2)	-0.0058	-0.0770
-1.0	58	0	-0.1026(2)	-0.0083	-0.0932

*ambrosetti@science.unitn.it

†pederiva@science.unitn.it

‡lipparin@science.unitn.it

§gandolfi@sissa.it

¹J. Nitta, T. Akazaki, H. Takayanagi, and T. Enoki, Phys. Rev. Lett. **78**, 1335 (1997).²G. Engels, J. Lange, Th. Schäpers, and H. Lüth, Phys. Rev. B **55**, R1958 (1997).³M. Kohda, T. Nihei, and J. Nitta, Physica E **40**, 1194 (2008).⁴E. I. Rashba, Phys. Rev. B **70**, 201309(R) (2004).⁵S. Datta and B. Das, Appl. Phys. Lett. **56**, 665 (1990).⁶E. Lipparini, *Modern Many Particle Physics*, 2nd ed. (World Scientific, Singapore, 2008).⁷I. L. Aleiner and V. I. Fal'ko, Phys. Rev. Lett. **87**, 256801 (2001).⁸M. Valín-Rodríguez, A. Puente, L. Serra, and E. Lipparini, Phys. Rev. B **66**, 165302 (2002).⁹A. Emperador, E. Lipparini, and F. Pederiva, Phys. Rev. B **70**, 125302 (2004).¹⁰L. O. Juri and P. I. Tamborenea, Phys. Rev. B **77**, 233310 (2008).¹¹R. S. R. C. Grimm, J. Comput. Phys. **7**, 134 (1971).¹²D. Ceperley and M. Kalos, *Monte Carlo Methods in Statistical Physics*, 2nd ed. (Springer, Berlin, 1979), p. 145.¹³D. Ceperley, Phys. Rev. B **18**, 3126 (1978).¹⁴B. Tanatar and D. M. Ceperley, Phys. Rev. B **39**, 5005 (1989).¹⁵A. Sarsa, S. Fantoni, K. E. Schmidt, and F. Pederiva, Phys. Rev. C **68**, 024308 (2003).¹⁶S. Gandolfi, A. Y. Illarionov, K. E. Schmidt, F. Pederiva, and S. Fantoni, Phys. Rev. C **79**, 054005 (2009).¹⁷F. Bolton, Phys. Rev. B **54**, 4780 (1996).¹⁸L. Colletti, F. Pederiva, E. Lipparini, and C. J. Umrigar, Eur. Phys. J. B **27**, 385 (2002).¹⁹S. Gandolfi, F. Pederiva, S. Fantoni, and K. E. Schmidt, Phys. Rev. Lett. **98**, 102503 (2007).²⁰S. Gandolfi, F. Pederiva, S. Fantoni, and K. E. Schmidt, Phys. Rev. Lett. **99**, 022507 (2007).²¹S. Gandolfi, A. Y. Illarionov, S. Fantoni, F. Pederiva, and K. E.

- Schmidt, Phys. Rev. Lett. **101**, 132501 (2008).
- ²²C. Lin, F. H. Zong, and D. M. Ceperley, Phys. Rev. E **64**, 016702 (2001).
- ²³Y. Xiao, M. F. Thorpe, and J. B. Parkinson, Phys. Rev. B **59**, 277 (1999).
- ²⁴C. Attacalite, S. Moroni, P. Gori-Giorgi, and G. B. Bachelet, Phys. Rev. Lett. **88**, 256601 (2002).
- ²⁵G. Dresselhaus, Phys. Rev. **100**, 580 (1955).